18th International Conference on Structural Mechanics in Reactor Technology (SMiRT 18)
Beijing, China, August 7-12, 2005
SMiRT18-P01-2

SIMPLIFIED MODEL OF PWR VESSEL TEARING UNDER SEVERE ACCIDENT CONDITIONS. APPLICATION TO LHF TESTS AND REACTOR SITUATIONS

Thomas LAPORTE
DEN/DM2S CEA SACLAY
91191 GIF-SUR-YVETTE Cedex, FRANCE
Phone: +33 1 69 08 95 57
Fax: +33 1 69 08 86 84
E-mail: tlaporte@cea.fr

Philippe MONGABURE
DEN/DM2S CEA SACLAY

ABSTRACT

Between 1999 and 2003, CEA conducted a R&D program on high temperature ductile tearing of French PWR vessel steel 16MND5. The main goal was to develop simplified high temperature tearing models, validated on experimental data, and allowing parametrical studies of various severe accident situations of vessel failure. These models are to give estimations of the final breach section (and therefore assess the risks of complete unzipping of the vessel), which are major safety concerns with regard to molten corium ejection and ex-vessel initial conditions.

The model presented in this paper concerns circumferential tearing and applies to fast opening situations, for which breach propagation is coupled to vessel depressurisation. Following an experimental program of high-temperature tearing tests on Compact Tensile specimens and Centre Crack Panels, a perfect plastic behaviour with a strain rupture criterion have been chosen, and simple assumptions were made on stress and strain distribution. The equations of the model are based on the energetic differential balance between the kinetic energy, the external work of the pressure load and the energy dissipated in the tearing process, coupled to an isothermal depressurisation model. This system is numerically solved to obtain the breach length and section versus time during the depressurisation process.

The application of this model to the LHF tests 3, 5 and 8 shown a very good agreement with the experimental results concerning the final breach size and the dynamic stability or instability of the structure. Dimensionless key parameters were identified, allowing simple assessments on the risks of catastrophic failure in experimental or reactor situations. Moreover, the importance of pressure history before failure was explained : lower and constant pressure values (implying creep failures) lead to dynamically stable situations and smaller breach sections, whereas fast plastic failures during pressure ramps lead to dynamically unstable situations and catastrophic failures may occur.

Finally, a PWR severe accident situation with corium relocation in the vessel bottom head has been modelled. The main result is that catastrophic failure (complete unzipping of the vessel bottom head, like in the LHF 5 test) can occur in situations of late vessel reflooding, leading to a re-pressurisation of the primary circuit at high vessel temperature. These situations are of low probability, but these results might have important consequences on accident management and safety assessments.

Keywords: PWR, Severe Accidents, Pressure Vessel, Ductile Tearing, Simplified Modelling.

1. INTRODUCTION

During a hypothetic severe accident in a PWR, with molten corium relocation into the vessel bottom head, and residual primary pressure (typically 10 to 20 bars), hot spot or weakened zone might lead to vessel creep or plastic failure. In this case, it is important to be able to predict the breach section during the vessel tearing (which may be coupled to depressurisation), and therefore the final breach section which is a major safety concern with regards to molten corium ejection and ex-vessel initial conditions.

Between 1999 and 2003, CEA conducted a R&D program on high temperature ductile tearing of French PWR vessel steel. This “Breach Program”, set up with EDF and Framatome in the framework of severe accident studies, was focused on the development of simplified high temperature tearing models, validated on experimental data, and allowing parametrical studies of various severe accident situations of vessel failure. This program consisted in :

- High temperature tearing tests on small specimens (500°C < T < 1000°C).
- High energy pipe burst tests at 700°C on circumferentially notched tubes with initial defect.
- Development of semi-analytical simplified models of ductile tearing.
- Tests interpretation calculations with CAST3M (finite elements code developed at CEA).
- Validation of the simplified models on existing tests.

The simplified model presented in this paper concerns circumferential tearing and applies to fast opening situations, for which breach propagation is coupled to vessel depressurisation.

When applied to LHF tests [LHF (1999)] for example (see part 5 for more details), this model has to be able to discriminate tests such as LHF 3, 5 and 8 (Figure 1), give an explanation of the complete unzipping of LHF 5, and assess the risks of complete unzipping of the vessel in reactor situations.

Figure 1 : Post-test view of LHF 3, 5 and 8 (from [LHF (1999)])

2. CONTEXT

Ductile tearing and dynamic crack propagation in pressurized vessels or piping are important research themes in the nuclear field [Kussmaul (1982)], but when this program was launched in 1998, apparently none of them had been investigated in the temperatures range reached in a PWR vessel during a severe accident. The RUPTHER [Devos (1998)] and LHF [LHF (1999)] campaigns would provide experimental results concerning high temperature tearing of PWR vessel steels, but were designed to study the behaviour until failure, and not the tearing phenomenon itself.

At high temperatures (T > 600°C), American or French PWR vessel steels are known to become very ductile, and therefore, the tearing occurs at very high levels of inelastic strains (for example in LHF tests [LHF (1999)], the local plastic strain currently reached $\varepsilon_p \sim 200$ % at failure initiation). In these situations, classical fracture mechanics methods could not be used anymore, and the tearing phenomenon itself had to be investigated before developing calculation models.

Therefore, a preliminary objective of the CEA Breach Program was to improve the knowledge on high temperature tearing of vessel steel.

3. AN OVERVIEW OF THE “BREACH PROGRAM” MAIN RESULTS.

3.1 Experimental findings.

During the RUPTHER campaign in CEA [Devos (1998)], the mechanical properties of French vessel steel 16MND5 were determined from room temperature to 1300°C with steps of 100°C. The specimens used for the tearing tests of the Breach Program were made of the very same sample of steel.

During the Breach Program, the following high temperature tearing tests were conducted at CEA-Saclay in the RESEDA facility :

- 2 tests on Compact Tensile specimens (CT) at 700 & 1000°C loaded with displacement ramps.
- 10 tests on Centre Cracked Panels (CCP) at 500, 600, 700 & 900°C loaded with effort ramps at variable ramp speeds from constant load to 60 MPa/min (fast ductile tearing).

All specimens were pre-cracked with a fatigue loading at room temperature. The main conclusions of this campaign were :

- The tearing behaviour becomes highly ductile between 600 and 700°C.
- At high temperatures (T > 600°C), no effect of pre-cracks can be observed.
- Between 700°C and 1000°C tearing occurs at extremely large local failure strains (300 to 400 % elongation in the necking zone), and its average value is nearly independent of the temperature.

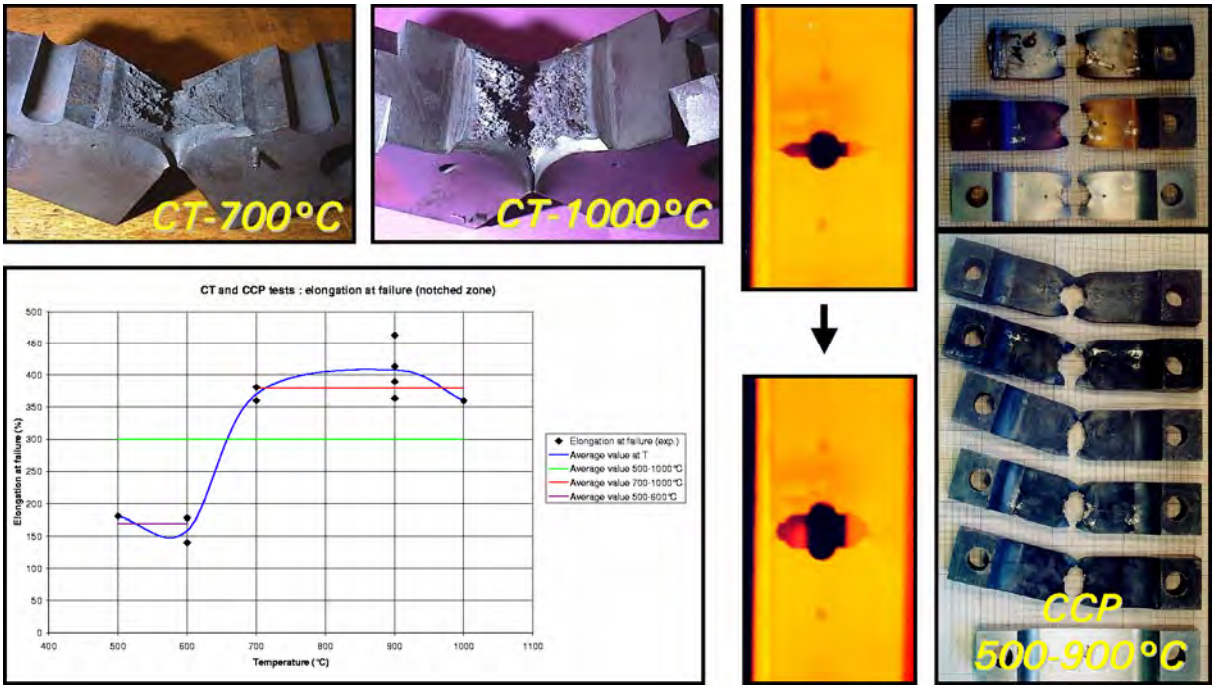

Figure 2 : Experimental results, CT and CCP tests

3.2 Modelling results.

The F.E. and simplified interpretation calculations of the tests led to the following conclusions :

- Failure criteria based on equivalent plastic strain allow good predictions of tearing tests.
- Accurate predictions of effort and displacement versus time during tearing tests requires F.E. 3D modelling, and cannot be achieved with simplified models.
- Nevertheless, a good global estimation of the energy dissipated during the tearing process can be obtained with simplified models.
- *Because of the very large failure strains and the very important necking, the surface rupture energy is negligible compared to the energy dissipated during the plastic deformation process.*

4. DESCRIPTION OF THE SIMPLIFIED MODEL.

4.1 Objective.

During a severe accident in a PWR, once molten corium is relocated into the vessel bottom head, the temperature field cannot be perfectly homogeneous, and therefore the vessel failure is to occur in a particularly weakened zone : hot spot or thickened zone (because of the inner melting of the vessel submitted to very high temperatures by the corium, and concentration of creep strains for example).

In case of vessel failure, it is important to be able to predict the breach section during the vessel tearing (which may be coupled to depressurisation), and therefore the final breach section which is a major safety concern with regards to molten corium ejection and ex-vessel initial conditions.

- In a situation of “hot spot failure”, the model must be able to assess if the breach will propagate outside the hot spot, and what its final section will be.
- In a situation of molten corium pool under natural convection (with an edge peaked temperature field), the model may be able to assess the risks of complete unzipping through an analysis of the dynamic stability of the structure and the possible initial breach sizes.

The simplified model presented in this paper has been developed for the case of circumferential tearing in cylindrical or hemispherical structures. Keeping in mind the various uncertainties of the severe accident context, and in order to be able to process wide parametrical studies, this simplified model has to process in a few seconds of CPU time.

This kind of tearing model is not designed to predict the mechanical behaviour of the structure *before* failure : the initial conditions of the tearing phenomenon *are* the conditions at failure.

4.2 Physical modelling.

Depressurisation through the breach is simulated with a perfect gas model expressed as following :

Equation 1 : $\boxed{\dot{P} = -K.S.P}$

With $K = \frac{1}{V}\sqrt{\frac{R_G.T}{M}}$

P : Pressure value.
S : Breach section.
V : Initial volume of pressurized gas in the structure.
T : Temperature of the gas.
R_G : Perfect gas constant.
M : Molar mass of the gas.

A derivative expression of the first principle of thermodynamics can be applied to the bottom head :

Equation 2 : $\boxed{\dot{E}_c + \dot{E}_{int} = \dot{E}_{ext}}$

E_{ext} : Work of external forces (pressure).
E_c : Kinetic energy of the bottom head.
E_{int} : Dissipated energy (deformation and tearing). Only plastic dissipation until failure is considered (surface rupture energy is neglected, Cf. §3.2).

With :

$$\dot{E}_c = \int_{V_{BH}} \rho.\dot{u}.\ddot{u}.dV$$

$$\dot{E}_{int} = \int_{V_S} \sigma.\dot{\varepsilon}_p.dV$$

$$\dot{E}_{ext} = \int_{S_P} P.\vec{\dot{u}}.\overrightarrow{dS}$$

V_{BH} : Volume of steel of the bottom head
V_s : Volume of steel affected by plastic deformation during the tearing process.
S_p : Surface subjected to pressure.
ρ : Vessel steel specific mass.
u : Displacement field.
σ : Stress tensor (*in this equation only*).
ε_p : Plastic strain tensor.

4.3 Equations of the simplified model.

4.3.1 Simplification of the physical problem.

The physical problem of ductile tearing coupled with depressurisation is completely defined by the system of Equations 1 and 2. In order to develop a simplified model for the circumferential tearing of a vessel bottom head at high temperature, and considering the findings of the Breach Program (part 3), this system can be simplified with the following hypotheses (see Figure 3) :

- Tearing mode : circumferential at a given latitude (angle ψ).
- Bottom head : hemispherical. Displacement field : rotation of the lower part (angle θ).
- Volume affected by plastic deformation during the tearing process : overheated zone.
- Temperature field : assumed to be constant in the tearing zone (except in the breach itself).
- Mechanical modelling : perfect plastic behaviour.
- Simplified strain distribution : the plastic strain is assumed to be linear as a function of the radius, from 0 (rotation axis) to the rupture strain (breach tip).

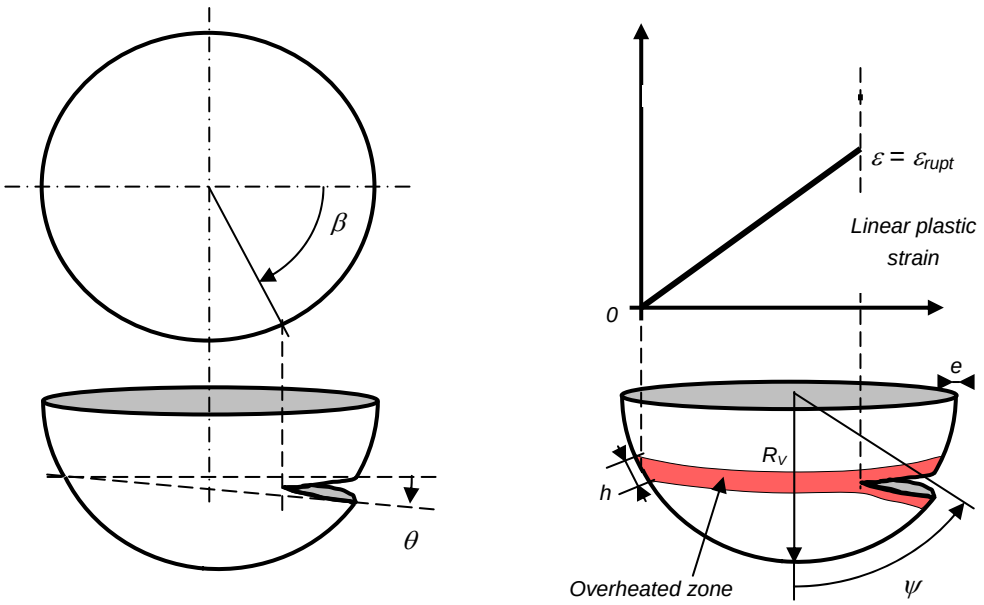

Figure 3 : Notation and assumptions of the circumferential simplified tearing model.

The following notations are used :

ψ	: Latitude of the overheated zone.	θ	: Angle of bottom head rotation.
R_V	: Vessel radius.	β	: Half centre angle of the breach.
R	: Vessel radius in the tearing plan ($\sim R_V.\sin\psi$).	h	: Height of the overheated zone.
e	: Vessel thickness : averaged value in the overheated zone at failure time.	ε	: Failure strain (at the average temperature value).

4.3.2 Relations between the system parameters.

With these hypotheses, any tearing state of the structure is completely defined by the variable θ, and *therefore, Equation 2 becomes a 2nd order differential equation of the variable θ and the whole problem is reduced to a system of two differential equations that can be numerically solved to obtain variables θ and P as a function of time.*

The relation between θ and β is obtained through the tearing criterion ε :

Equation 3 :
$$\tan\frac{\theta}{2} = \frac{1}{2}\frac{h.\varepsilon.\sin\psi}{R.(1+\cos\beta)}$$

At a given longitude, the breach opening is the difference between the total elongation ($h + \Delta h$) and the elongation at rupture ($h + \Delta h_{rupt} = h.(1+\varepsilon)$). Integrating the breach opening between longitudes $-\beta$ and β gives the expression of the breach section :

$$S(\beta) = \frac{2R.h.\varepsilon.(\sin\beta - \beta.\cos\beta).\sin\psi}{(1+\cos\beta)}$$

This value has of course to be limited to the maximum value $S_{max} = \pi.R^2$.

4.3.3 Energetic terms.

Considering a rotational motion of the vessel bottom head (typically observed in LHF 5), described by the angle θ, analytical expressions of the energetic terms can be obtained :

$$\dot{E}_c = \int_V \rho.\dot{u}.\ddot{u}.dV = J_{tot}.\dot{\theta}.\ddot{\theta}$$

With $J_{tot} = \pi.\rho.e.R_V^4\left(\frac{10}{3} - 5\cos\psi + \frac{5}{3}\cos^3\psi\right)$ (inertial momentum of the bottom head)

Power of the pressure load : $\dot{E}_{ext} = \int_S P.\vec{u}.\overrightarrow{dS} = P.\pi.R^3.\dot{\theta}$

The dissipated power in the deformation and tearing process is obtained by the integration of the plastic dissipated power in the non-breached part of the overheated zone

$$\dot{E}_{int} = 2.e.h.R.\sigma.\varepsilon \frac{(\pi - \beta - \sin\beta).\sin\beta}{(1+\cos\beta)^2}\dot{\beta}$$

σ is a reference stress such as $\sigma.\varepsilon$ is the volumic dissipated energy until failure. The value of $\sigma(T)$ has to be identified on dedicated tearing tests. Otherwise, the ultimate strength of the material can be used.

Using Equation 3, $\dot{E}_{int}$ is easily expressed as a function of θ.

4.4 Mechanical consequences on the structural behaviour.

4.4.1 Tearing initiation condition.

At the initial time, motion and tearing start only if $\dot{E}_{ext} > \dot{E}_{int}$, hence the tearing initiation condition :

Equation 4 : $$P_0 > \frac{2\sigma.e}{R.\sin\psi}\left[1-\frac{\beta_0}{\pi}-\frac{\sin\beta_0}{\pi}\right].\left[1+\left(\frac{h.\varepsilon.\sin\psi}{2R.(1+\cos\beta_0)}\right)^2\right]$$ (β_0 : initial breach size)

This condition is expressed here as a limit pressure, but for a given pressure value P_0, Equation 4 implicitly defines a limit size β_{lim} for the initiation of unstable breach propagation.

This condition can be interpreted as a static stability criterion at P_0 as follows :

The first term represents mechanical stability in the horizontal plane at latitude ψ with no breach. The second term accounts for the stress increase because of the breach (section reduction and moment).

Using Equation 3, the last term becomes : $$\left[1+\left(\frac{h.\varepsilon.\sin\psi}{2R.(1+\cos\beta_0)}\right)^2\right] = \frac{1}{\cos^2\frac{\theta}{2}}$$

This accounts for the potentially important values of θ at failure, because of the very large failure strain at high temperature.

4.4.2 Dynamic stability.

Tearing starts because of a static instability of the structure. Then, the system happens to be either "*dynamically stable*" if the cumulated effects of the inertia of the bottom head and of depressurisation lead to a new equilibrium with a limited breach propagation, or "*dynamically unstable*" if despite these effects, the structure remains unstable and a complete unzipping occurs.

Dynamic stability depends on the level of coupling between breach propagation and depressurisation, and therefore depends on all the parameters of the system. In a closed system (no depressurisation), dynamic stability can be estimated by comparing the potential energy (gas under pressure) and the energy that can be dissipated in the structure (plastic dissipation).

When the situation is dynamically very stable (fast depressurisation, hardly no tearing) or very unstable (complete unzipping before significant pressure drop) the level of coupling is very low and the dynamic stability criterion can be obtained by comparing the mechanical energy transferred to the structure by a complete adiabatic pressure drop and the energy dissipated in the complete unzipping of the bottom head (γ : specific heat ratio of the gas) :

Dynamic stability criterion :

$$\lambda = \frac{2\pi.R.h.e.\sigma.\varepsilon.(\gamma-1)}{P_0 V_0}$$

$\lambda >> 1$ → the structure is dynamically very stable.

$\lambda << 1$ → the structure is dynamically very unstable.

5. APPLICATION TO LHF TESTS 3, 5 & 8.

5.1 A brief description of the tests.

LHF tests [LHF (1999)] consisted in simulating a severe accident in a PWR vessel bottom head scaled at 1:4.85 and made of SA533B1 American vessel steel. The vessels were pressurized to a constant value (10 MPa), and submitted to a temperature ramp until failure. LHF tests number 3, 5 and 8 were conducted with an edge-peaked temperature distribution corresponding to the heat flux of a convecting molten corium pool.

The most interesting difference between those tests is that a limited circumferential rip occurred in tests LHF 3 & 8, at ~1000 K whereas in test LHF 5, an unplanned pressure transient at ~1000 K (leakage down to 7 MPa followed by a re-pressurisation at 10 MPa) led to a dramatic failure with a complete circumferential unzipping of the vessel at ~1100 K (see Figure 1).

Post tests analyses indicated that in tests LHF 3 and 8, failure occurred because of a visco-plastic instability with no definite precursor, whereas in test LHF 5 a zone of roughly 20° of longitude located at the initial failure site displayed the saw-tooth edge characteristics of tensile failure.

It is important to notice that different heating systems were used along the LHF campaign, inducing variations of the overheated zone properties between the tests : a radiative heater with isolating fences was used for LHF 3, whereas an inductively heated graphite cavity was used in LHF 5 and 8 (two different designs : larger cavity height in LHF 8). As a result, the overheated zone of test LHF 5 happened to be smaller in height than in LHF tests 3 and 8, with a larger azimuthal temperature variation in the overheated zone.

5.2 Analysis method.

As LHF tests were conducted with inhomogeneous 3D temperature fields on mock-ups with no initial defects, the initial breach size (used in the model) cannot be defined precisely because :

- It cannot be measured post-mortem as propagation occurred.
- It depends on the global behaviour and on local 3D effects in the neighbourhood of the initial failure site, what can only be calculated with 3D F.E. modelling and cannot be determined simply.

Therefore, knowing the pressure and temperature field at failure time, the propagation limit size is calculated using Equation 4 and compared to the final breach size (or to the initial size for LHF 5).

Dynamic stability is first roughly estimated with the simple criterion λ defined above, and then more precisely by processing calculations for increasing values of the initial breach length.

5.3 Model parameters.

All parameters of the simplified tearing model have been estimated using experimental data available in the LHF NUREG report [LHF (1999)]. Experimental data and parameters estimation are described below. Their values are summarized in Table 1.

5.3.1 Depressurisation model.

In all tests, the gas was Argon (M = 40 g/mol ; γ = 1.66) and failure conditions were assumed to be :

Pressure : $P_0 = 100$ *bars ;* Volume of gas : $V_0 = 0.2\ m^3$; Gas temperature : $T = 1000K$

Therefore, the value of the depressurisation constant K (see §4.2) is : $K = 2280\ m^{-2}s^{-1}$

5.3.2 Mechanical model.

As described in 4.3.1, thickness and temperature values are averaged in the overheated zone, outside the initial breach, and the *real* radius in the tearing plan at failure time is used (therefore its value is not exactly $R_V.sin\psi$ because vessel deformation is taken into account).

As no tearing tests are available, the ultimate strength at the averaged temperature is obtained using correlations given in [LHF (1999)] for the LHF SA533B1 steel, and the failure strain is set to the estimated value of : ε = 200% [LHF (1999)].

The height of the overheated zone (*h*) is estimated on the basis of :

- The heater properties (heating height).
- The latitudinal temperature and yield stress fields at failure time

These estimations were successfully correlated with measurements of vessel post-test thickness distributions, what confirmed that in these tests, the overheated height was close to the height affected by plastic deformation. These values of *h* points out the important differences between the heating systems used in these three tests :

- The radiative heater used in LHF 3 overheated the vessel on ~15-20° of latitude, what led to an overheated height of ~16 cm.
- The first design of the inductively heated radiative cavity used in LHF 5 led to a very narrow latitudinal temperature peak with a height of ~4 cm.
- The final design of this system (with enlarged cavity) led to a wider temperature peak of ~12 cm.

One can also notice that the vessel radius in the tearing plan also reflects this difference :

- In LHF 5, this radius is very close to the initial radius ($R = 37.5\ cm$, and $R_V.\sin\psi = 37.2\ cm$), what is significant of a creep deformation strictly localized in the temperature peak zone.
- In LHF 3 and 8, a more global deformation of the vessel bottom head was induced by the larger overheated height.

Table 1 : Values of the model parameters for tests LHF 3, 5 & 8.

	R (cm)	e (cm)	h (cm)	σ (Mpa)	ε (%)	ψ (°)	J (kg.m^2)	K (m^{-2}.s^{-1})
LHF 3	41	2.5	16	109	200	55	23	2280
LHF 5	37.5	1.7	4	80	200	55	23	2280
LHF 8	43	2.6	12	108	200	67	46	2280

5.4 Results.

The main results are summarized in Table 2 and analysed below.

Table 2 : LHF 3, 5 and 8 : Comparison between calculated and experimental results.

		LHF 3	*LHF 5*	*LHF 8*
Stability criterion	λ	0.75	0.085	0.6
Breach limit size	$2.\beta_{lim}$ (°)	75	16.4	56.6
	$2.\beta_{exp}$ (°)	75	20 → 180	50
Final breach section	S_{calc} (cm^2)	107	4417	27
	S_{exp} (cm^2)	135	4428	28
Post-test view of the LHF vessel bottom head	*Exp.*	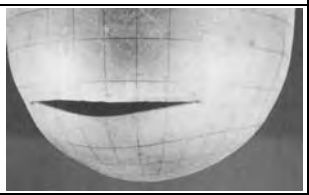		
	Model	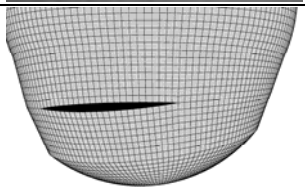	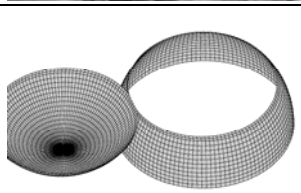	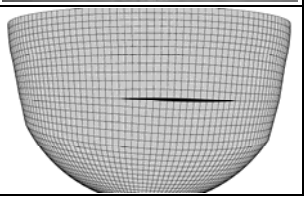

5.4.1 Dynamic stability criterion.

As shown in Table 2, the values calculated for λ indicate that at failure time, LHF 5 was very dynamically unstable ($\lambda << 1$), and that LHF 3 and 8 were much more stable than LHF 5. This result is coherent with experimental results.

Nevertheless, the values of λ for LHF 3 and 8 are close to $\lambda = 1$, and do not allow any accurate conclusion on dynamic stability.

5.4.2 Propagation limit size.

The propagation limit size is calculated using Equation 4, and gives the initial breach size over which dynamic tearing may occur. *For symmetry reasons, the variable β is the half centre angle of the breach, therefore, the propagation limit size of the breach is 2.β_{lim}.* For LHF 5, the angular length of the initial tensile failure zone (see 5.1) is also reported in Table 2.

Considering the simplicity of this estimation, the result for LHF 3 (identical values of β_{lim} and β_{exp}) does not have any special meaning, except that like in LHF 8, the experimental final breach size is close to the calculated propagation limit size. This implies that dynamic stability has to be studied with the model in order to obtain a significant result.

For LHF 5, this result is much more significant, because the initial failure zone is larger than the propagation limit size. This means that a dynamic tearing may occur outside this initial failure. As we know that the structure is dynamically very unstable ($\lambda << 1$), these two parameters let us predict a complete unzipping of the vessel bottom head, as experimentally observed.

5.4.3 Estimations of breach section.

In the model, the breach section estimation is based on the hypotheses of failure strain criterion and linear plastic strain distribution (see § 4.3.2), and only depends on the parameters β, R, h, and ε. Therefore, the experimental final breach section (S_{exp}) can be compared to the breach section (S_{calc}) calculated with the <u>*experimental value β_{exp}*</u>, what allows a stand alone validation of these hypotheses.

For LHF 5, the final breach section is $\pi.R^2$, and therefore very easily estimated.

For LHF 3 and 8, the experimental section is estimated with a good accuracy.

This implies that the hypotheses of linear distribution of plastic strain in the overheated zone and failure strain criterion seem to simulate accurately the experimental tearing behaviour of the structure. Pictures in Table 2 were generated by deforming a mesh of the LHF bottom head following only and strictly the model hypotheses with the parameters and results of Table 1 and Table 2.

5.4.4 Dynamic calculations with the simplified model.

<u>*LHF 3*</u> *:*

As shown in Table 2, β_{lim} = 37.5°. For β_0 < 37.5°, there is no propagation outside the initial breach.

For β_0 = 40°, a limited propagation is obtained, with a final breach half-size of β_{fin} = 47°, and a final breach section of 210 cm^2. At the end of propagation, the pressure is still at a high value of 81 bars.

For β_0 = 50°, a very important propagation is obtained, with a final breach half-size of β_{fin} = 111°. After complete depressurisation of the structure, the propagation stops with no complete unzipping.

These results reflects the well balanced energy ratio (λ ~ *1)* : even for a large initial breach, there is not enough energy in the pressurized gas to tear the whole structure. With regards to the simplicity of the model, one can conclude that the creep failure of LHF 3 remained localized to the initially weakened zone, and no plastic propagation occurred outside this zone.

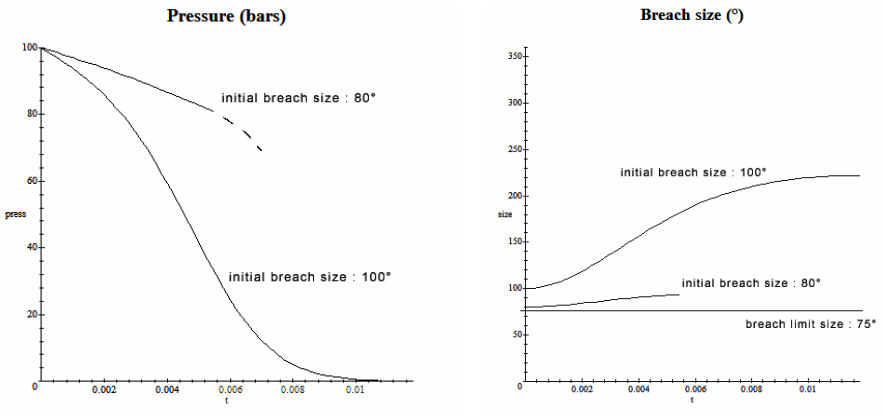

Figure 4 : LHF 3, calculated pressure and breach size versus time (s).

LHF 5 :

As shown in Table 2, β_{lim} = 8.2°. For β_0 < 8.2°, there is no propagation outside the initial breach.

For β_0 = 8.5°, the vessel bottom head is completely unzipped in a few milliseconds, and after the vessel complete depressurisation (~13 ms), the bottom head rotation speed is still very important.

This result reflects the very important dynamic instability of the structure (λ << *1*), and is completely coherent with the experimental result.

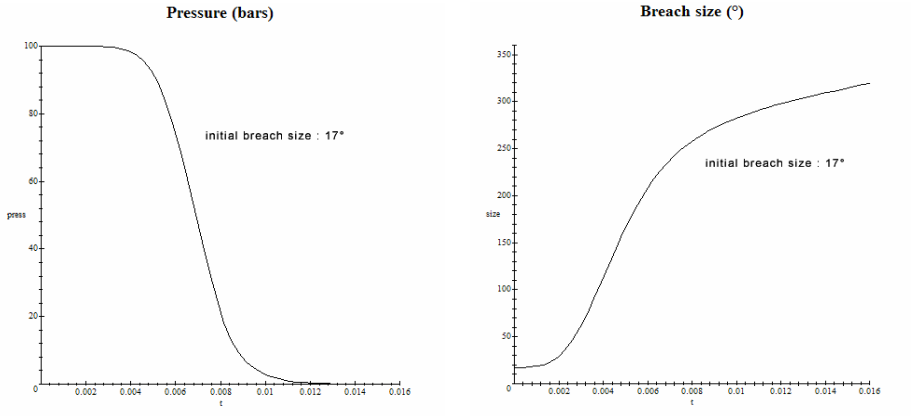

Figure 5 : LHF 5, calculated pressure and breach size versus time (s).

LHF 8 :

As shown in Table 2, β_{lim} = 28.3°. For β_0 < 28.3°, there is no propagation outside the initial breach.

For β_0 = 29°, a very limited propagation is obtained, with a final breach half-size of β_{fin} = 29.4°, and a nearly constant breach. At the end of propagation, the pressure is still at a very high value of 97.5 bars.

For β_0 = 30°, an important propagation is obtained, with a final breach half-size of β_{fin} = 126°. Nevertheless, after the complete depressurisation of the structure, the propagation stops with no complete unzipping.

These results are very similar to LHF 3 and lead to the same conclusions : failure remained localized to the initially weakened zone, and no plastic propagation occurred outside this zone.

5.4.5 Analysis of LHF tests 3, 5 & 8.

The results obtained in this analysis are in good agreement with the experimental results, and suggest that the tearing behaviour of LHF tests can be simulated with an energetic approach of ductile tearing coupled with depressurisation.

As a result, the much smaller overheated height and lower ultimate strength (because of a higher failure temperature) are important parameters that explain the catastrophic failure of LHF 5. The limited breach propagations observed in tests LHF 3 & 8 can also be predicted, and rough estimations of final breach length can be achieved. More accurate values would require pre-calculation of the global behaviour before failure with another model (3D F.E. for example). The hypothesis of linear plastic strain distribution with a failure strain criterion allow an accurate estimation of the breach section for a given breach length.

6. APPLICATION TO A REACTOR ACCIDENTAL SITUATION.

In this part, an application of the model to a PWR accidental situation is presented. The main objective here was to estimate the risks of catastrophic failure (LHF5-like) in a realistic situation, through a parametric study of the vessel bottom head tearing.

6.1 Scenario, parameters.

Considering a French PWR 900 MWe, in-vessel retention is not a accident management strategy, therefore only situations *without external cooling* were *studied. In this case, important breach sections are mainly a problem with regards to Direct Containment Heating. Therefore, critical situations correspond to relatively high pressure (~10 to 20 bars) and significant amount of liquid corium in the

bottom head (more than 20 tons).

Scenario estimations conducted in the framework of the “GAREC” (French CEA-EDF-Framatome workgroup on severe accidents), show that this situation is of low probability (the most probable failure mode is a vessel melting at low pressure). These estimations also show that some realistic scenarios could nevertheless lead to a mechanical failure of the vessel bottom head in these conditions : a first corium flow from the core in residual water, followed by a second corium flow 30 minutes later, leading to 20 to 30 tons of liquid corium above a debris bed of 20 to 30 tons.

At this point, the pressure in the primary circuit was considered to be 10 bars, with the possibility that a late vessel reflooding could lead to a fast re-pressurisation to 20 bars in a few minutes. With regards to the amount of corium, and the residual power, this situation conducted to a rather axisymmetrical overheated zone at the latitude $\psi = 60°$ with a through thickness thermal flux of 0.25 to 0.75 MW/m^2. For this level of heat flux, the permanent thermal state corresponds to a reduced vessel thickness because melting occurs at the vessel steel / corium interface.

The following parameters were used for the RPV :

Initial vessel thickness : 16 cm	$R_V = 2\ m$	Tearing criterion : $\varepsilon = 3.8$ (see Figure 2)
Depressurisation coefficient :	$K = 6.7\ m^{-2}.s^{-1}$	(100 m^3 of steam at 700°C)
Inertial momentum :	$J_{tot} = 210.10^3\ kg.m^2$	(bottom head below $\psi = 60°$ + 40 t of corium)

6.2 Simplified modelling of vessel failure.

In order to set the initial conditions of the tearing model (pressure, temperature, vessel thickness at failure), vessel failure had to be studied with a dedicated model. Considering the need of a parametrical study, a simplified model was chosen, keeping in mind the necessity to take into account the possibility of failure during fast pressure transients.

6.2.1 Material properties.

At very high temperature, viscoplasticity phenomena are very important and creep models are currently used to study the mid to long-term behaviour of RPV submitted to moderate pressure loads. Nevertheless, for fast pressure transient leading to shorter term vessel failure, creep models are out of there domain of validity, and predictions become less accurate.

Based on a very important campaign of creep tests and tensile tests at various strain rate conducted in CEA on French vessel steel 16MND5 (RUPTHER program [Devos (1998)] and FP4 project REVISA [Devos (2002)]), we chose to use a simple material modelling based on the admissible stress for a given loading mode.

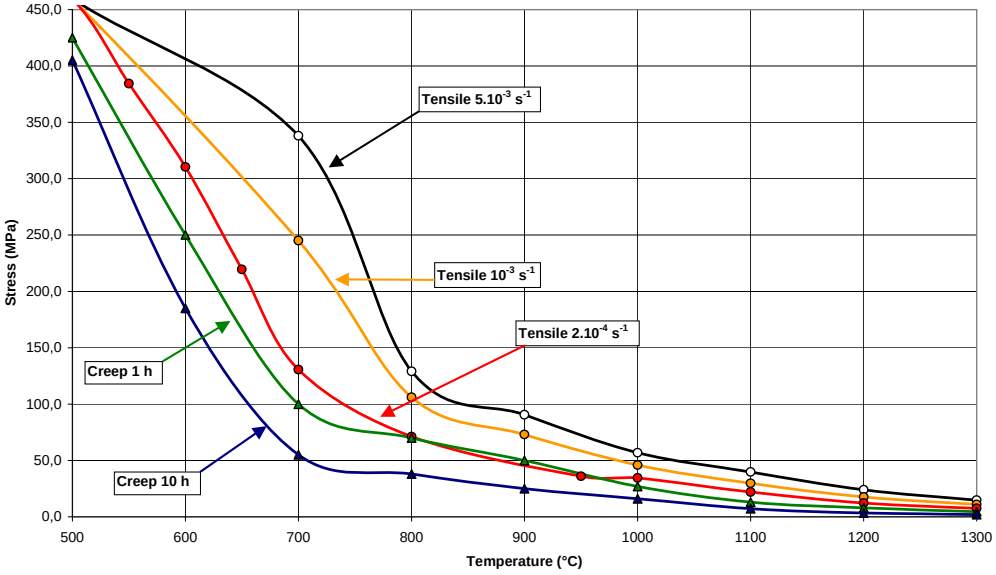

Figure 6 : Admissible stress versus temperature for different types of load.

On Figure 6 the maximum admissible stress is represented versus temperature for different kinds of failure mode : “creep” curves correspond to the initial stress of a creep test leading to failure in 1 h or 10 h, whereas “tensile” curves gives the mechanical resistance of the material (maximum stress of the engineering curve) in a tensile test at a given strain rate (2.10^{-4}, 10^{-3} and 5.10^{-3} s^{-1}).

Because of the very high ductility at high temperature, tensile tests at a strain rate of 2.10^{-4} s^{-1} last 30 to 60 minutes and the mechanical resistance of the material can be very close to the initial stress of a one-hour-failure creep test. On the other hand, in tensile tests at a strain rate of 5.10^{-3} s^{-1} failure is reached in 3 to 5 minutes, which is much more representative of what happens during a fast pressure transient (typical of a late vessel reflooding, but also representative of the unplanned pressure transient of the LHF 5 test).

6.2.2 Simplified thermo-mechanical model of vessel failure.

In order to take into account the different failure modes (slow/creep and fast/tensile) and the possible ablation of vessel thickness (because of inner melting), a very simplified model has been used.

Mechanical failure is based on the stress level compared to the admissible stress described previously. The stress field is based on an hemispherical distribution, with a value depending on vessel thickness, which is calculated supposing a permanent thermal regime through the vessel wall :

$$P_{fail} = \frac{2e}{R_V}\sigma_{adm}$$

$$\varphi = \lambda_{th}\frac{\Delta T}{e}$$

P_{fail} : Pressure value at failure — *P_{fail} = 10 or 20 bars*

e : Vessel residual thickness

σ_{adm} : Admissible stress

λ_{th} : Thermal conductivity — *λ_{th} = 30 W/m/°C*

$\Delta T/e$: Through thickness thermal gradient

Considering the thermal flux levels (0.25 to 0.75 MW/m^2), vessel melting always occur, and therefore the inner temperature is set to T_{melt} = *1500°C*. Supposing a linear temperature distribution, the thermal equation gives a relation between average temperature and residual thickness for a given thermal flux.

Then, for a given pressure and a given failure mode, the mechanical equation gives a relation between thickness and admissible stress (at the average through thickness temperature).

For a clear illustration of the global tendency from long term creep failure to short term tensile failure, we studied three typical failure modes : “10 h failure”, “1 h failure” and “5 min failure”, corresponding respectively to the admissible stress values of “10 h creep failure”, “1 h creep failure or 2.10^{-4} s^{-1} tensile failure”, and “5.10^{-3} s^{-1} tensile failure” (based on the notations used in Figure 6).

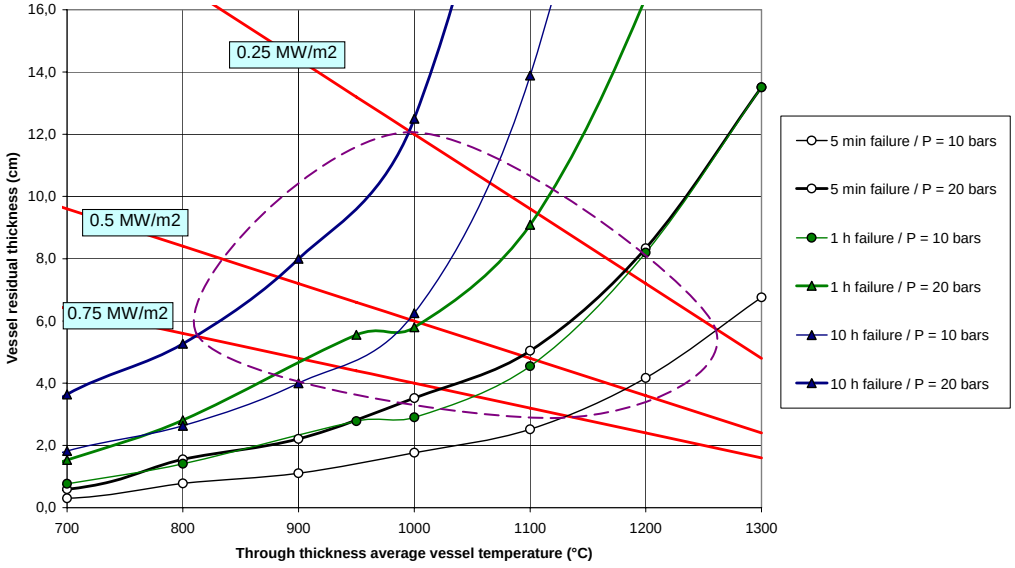

Figure 7 : Vessel failure conditions for different failure modes and thermal flux.

Considering the uncertainties inherent to the level of simplicity of this model, we studied the case “10 h failure”, even if not fully compatible with the hypotheses of the studied scenario (see §6.1). These “times to failure” are of course orders of magnitude, and could be better estimated with more sophisticated modelling.

The results of this analysis is shown on Figure 7 (red lines : thermal equation, blue, green and black curves : mechanical equation, purple dotted line : global failure domain).

Finally, based on this analysis, the vessel failure parameter range used for the tearing study is :

P = 10 ; 20 bars *800°C < T < 1250°C* *e = 3 → 12 cm*

6.3 Analysis of vessel tearing.

6.3.1 Stability criterion and breach limit size.

Based on the possible failure conditions described above, the possible values of λ (dynamic stability criterion) and β_{lim} (breach half limit size) were computed (Figure 8 and Figure 9), assuming a value of h = 30 cm (according to the amount of liquid corium in the scenario : 15 < h < 45 cm).

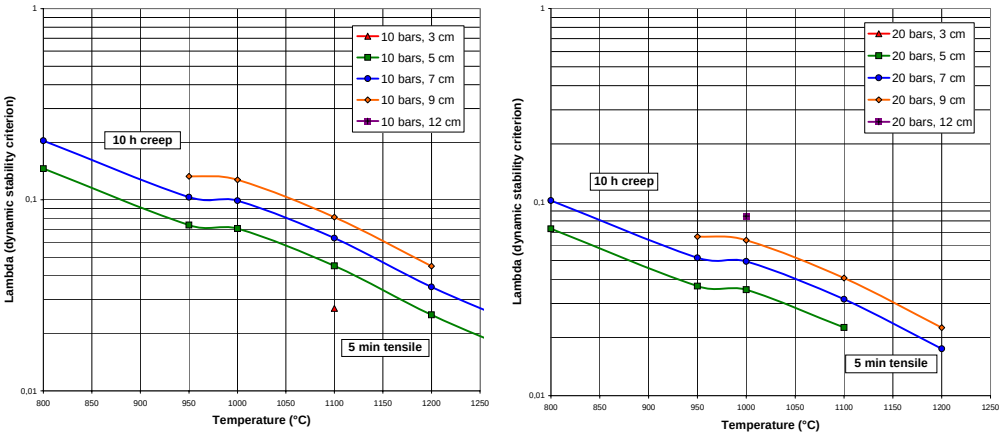

Figure 8 : Dynamic stability criterion for the reactor application.

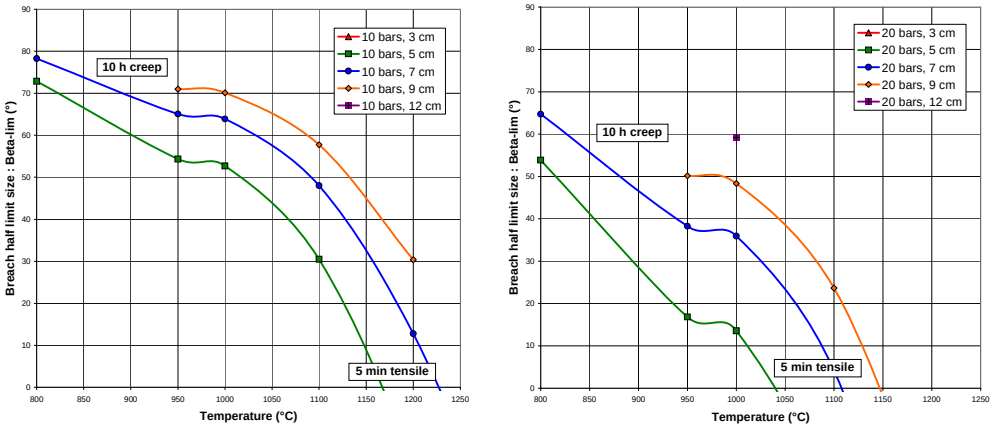

Figure 9 : Breach half limit size for tearing initiation (reactor application).

The main result of this analysis is that very critical situations ($\lambda < 0.1$ and $\beta_{lim} < 20°$) can be obtained at 10 and 20 bars for higher failure temperature and lower values of thickness. These failure conditions are to be found mostly in “5 min failure” situations, but also in some “1h failure” situations.

At 10 bars, the number of critical situations is smaller because the breach half limit sizes are bigger. Even with low values of λ, when $\beta_{lim} > 40°$, the initiation of tearing is very unlikely to occur as initial breaches of this size are very improbable (an 80° breach is 2.5 meters long).

6.3.2 Dynamic tearing calculations.

At this stage, a deeper analysis has to be done in order to have a better estimation of the transition between dynamically stable ($\lambda >> 1$) and unstable ($\lambda << 1$) situations, as most failure conditions are in the range $0.05 < \lambda < 0.2$.

Six typical situations have been studied, corresponding to the values of Table 3. Calculations were done in each case for two different values of the initial breach size *:* $\beta_0 = \beta_{lim} + 2°$ and $\beta_0 = \beta_{lim} + 10°$

Table 3 : Vessel failure conditions used in the dynamic tearing calculations.

Failure conditions	10 bars ; 0.5 MW/m^2			20 bars ; 0.5 MW/m^2		
	10 h failure	1 h failure	5 min failure	10 h failure	1 h failure	5 min failure
T	1000°C	1100°C	1200°C	900°C	1000°C	1100°C
e	6 cm	4.5 cm	4 cm	7.5cm	6 cm	5 cm
λ	0.085	0.04	0.02	0.09	0.04	0.022
β_{lim}	65°	24°	0°	58°	27°	0°
σ (MPa)	34.5	22	12.2	47	34.5	22

The results of this analysis is (see Figure 10 for breach section versus time in typical case) :

- In the “10 h failure” case, breach limit sizes are very important (Table 3). Initial breaches of this size are very improbable, and should they occur, dynamic tearing is still very limited. Practically, the breach would be limited to its initial size after creep failure. Precise prediction of this kind of breaches requires 3D finite elements calculations and the knowledge of the 3D thermal fields along the whole creep process (see [Nicolas (2002)] for example).
- In the “1 h failure” case, breach limit sizes are intermediate (similar to LHF 8), initial breaches of this size are realistic. Strictly speaking, dynamic tearing is limited (propagation stops), but final sections are always very important (close to the maximum value of $\pi.R^2 = 9.4$ m^2).
- In the “5 min failure” case, breach limit sizes are $\beta_{lim} = 0°$ (which means that failure occur in conditions close to the global plastic instability of the bottom head). Therefore any initial breach initiates dynamic tearing. Tearing is systematically highly unstable : very fast complete unzipping of the bottom head, with residual rotational kinetic energy.

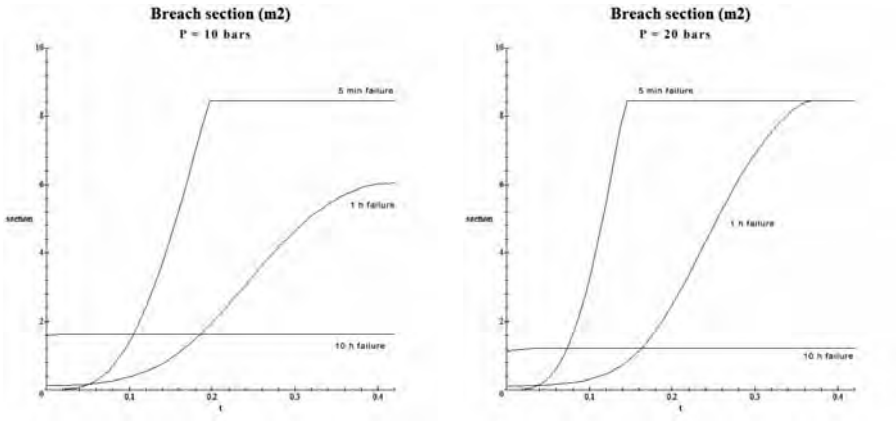

Figure 10 : Breach section (m^2) versus time (s) for different failure mode (PWR)

6.3.3 Analysis of the reactor case results

These results underlines that the final breach section is highly dependant on the very precise temperature and pressure conditions at failure, and particularly the negative effect of pressure transients at high temperatures can be explained by using a vessel failure model taking into account the possibility of short-term failure : for short term vessel failure, the *local* failure of the initial breach

occurs in condition that are much closer from the *global* plastic instability of the vessel bottom head.

These results also allow a better understanding of the LHF 5 test result by explaining the effect of the unplanned pressure transient at high temperature. Even without numerical data on the high strain rate tensile behaviour of the American vessel steel SA533B1, the tendency would obviously remain the same as it is a direct consequence of the decreasing importance of visco-plasticity at higher strain rate.

Moreover this effect was confirmed later on SA533B1 in an experimental campaign [OLHF (2003)] on rather similar vessel bottom heads : OLHF tests 1 and 2 were submitted to constant pressure loads (P_1 and $P_2 < P_1$ respectively), leading to small breaches in both cases, whereas the OLHF 3 test (dedicated to the pressure transient effect) was submitted to a planned pressure transient at high temperature from P_2 to P_1, leading to a catastrophic failure.

From the safety point of view, these results show that in realistic accidental conditions (but of very low probability), a complete unzipping of the vessel bottom head (LHF5-like) cannot be excluded in case of "late vessel reflooding" (that may cause a re-pressurisation at high temperature).

7. CONCLUSION.

In the framework of an experimental and modelling program on high temperature tearing of PWR vessel steel under severe accident loading conditions (Breach Program at CEA-Saclay), a simplified model has been developed to study breach propagation coupled with depressurisation.

Using an energetic approach of ductile tearing coupled with a perfect gas depressurisation law, this simplified model is based on a failure strain criterion, and linear plastic strain distribution in the zone affected by plastic deformation. Dimensionless key parameters has been identified, allowing simple assessments on the risks of catastrophic failure in experimental or reactor situations.

The application of this model to LHF tests 3, 5 & 8 allowed the identification of thermo-mechanical differences and similarities between these tests with regards to the tearing phenomenon. The limited tearing in LHF 3 and 8, and the complete unzipping of LHF 5 could be predicted with analytical criteria of dynamic stability and propagation limit size. The catastrophic failure observed in test LHF 5 could be explained by the unplanned pressure transient at high temperature.

Then, a vessel failure model taking into account short term failure (a few minutes on fast pressure transient for example) was used in order to obtain the initial conditions for the dynamic tearing process in various PWR failure conditions. Parametrical reactor studies conducted with the dynamic tearing model (on a French 900-MWe PWR basis) confirmed that the final breach section was highly dependant on the very precise temperature and pressure conditions at failure, and particularly the effect of pressure history before failure was explained : lower and constant pressure values (implying creep failures) lead to dynamically stable situations and smaller breach sections, whereas fast plastic failures during pressure ramps lead to dynamically unstable situations and catastrophic failures.

The main result is that complete unzipping of the vessel bottom head (LHF5-like) can occur in some specific scenarios leading to a re-pressurisation of the primary circuit at high vessel temperature (late vessel reflooding following two successive corium flow). These situations are of low probability, but these results are important for accident management and safety assessments.

8. REFERENCES

[1] [LHF (1999)] "*Lower Head Failure Experiments and Analyses"*, NUREG/CR-5582 – SAND98-2047

[2] [Kussmaul (1982)] "The effect of pipe burst investigations on the postulation of cracking in the primary cooling systems in light water reactors", K. Kussmaul & al., ASME PVP New York 1982, Vol. 94 p. 27-62, and "Experimental investigation on the crack opening behaviour of cylindrical vessels under light water reactor service conditions", K. Kussmaul & al., ASME PVP New York 1982, Vol. 62.

[3] [Devos (1998)] "The RUPTHER Program : Progress Status", J. Devos, P. Mongabure, C. Sainte-Catherine, L. Nicolas. ASME PVP San Diego, July 1998.

[4] [Devos (2002)] "REVISA, Final report (Extended Version)", J. Devos & al., INV-REVISA(01)-P006 / CEA Report Réf. SEMT/DIR/RT/02-002/A, April 2002.

[5] [Nicolas (2002)] "Failure propagation simulation in a RPV lower head under severe accident loading conditions", L. Nicolas & T. Locatelli, OLHF Seminar, Madrid, June 2002

[6] [OLHF (2003)] OECD-NEA : « OLHF Seminar 2002 », *Nuclear Safety NEA/CSNI/R(2003)1, 2003.*

